American Mineralogist, Volume 85, pages 1307–1314, 2000

Description and crystal structure of cabalzarite $Ca(Mg,Al,Fe)_2(AsO_4)_2(H_2O,OH)_2$, a new mineral of the tsumcorite group

JOËL BRUGGER[1,*], NICOLAS MEISSER[2], KURT SCHENK[3], PETER BERLEPSCH[4], MICHEL BONIN[3], THOMAS ARMBRUSTER[5], DANIEL NYFELER[5], AND SUSANNE SCHMIDT[4]

[1]VIEPS, Department of Earth Sciences, Monash University, VIC-3800 Australia
[2]Geological Museum and Institute for Mineralogy and Geochemistry, University-BFSH 2, 1015 Lausanne, Switzerland
[3]Institute for Crystallography, University of Lausanne, BSP, 1015 Lausanne, Switzerland
[4]Institute for Mineralogy and Petrography, University of Basel, Bernoullistrasse 30, 4056 Basel, Switzerland
[5]Laboratory for Chemical and Mineralogical Crystallography, University of Bern, Freiestrasse 3, 3012 Bern, Switzerland

ABSTRACT

Cabalzarite, $^{M1}Ca^{M2}(Mg,Al,Fe^{3+})_2(^{X}AsO_4)_2(H_2O,OH)_2$, is a new mineral of the tsumcorite group occurring in altered Mn ore at the abandoned Falotta mine (Swiss Alps). Together with other arsenates, cabalzarite documents the mobility of As during the retrograde stage of the Tertiary Alpine metamorphism under lowest to sub-greenschist facies conditions. Cabalzarite crystals vary in morphology from hatchet-like to fibrous and tabular. The color is light-brownish to salmon pink or orange brown, and the average refractive index is around 1.7. Cabalzarite is chemically inhomogeneous, with the main variations occurring on the octahedral M2 site occupied by Mg, Al, Fe^{3+}, and Mn^{3+}. Al and Mg are the dominant M2 cations, with Al/(Al + Mg) ratios varying between 0.31 and 0.59 (92 analyses). Cabalzarite is the first member of the tsumcorite group with octahedral Mg and Al as major constituents. Single-crystal X-ray structure refinements were performed on two different crystals. Cabalzarite is monoclinic, space group *C*2/*m*, Z = 2. The cell parameters for the type crystal CABA11.5, of composition $(Ca_{1.00}Sr_{0.02})(Al_{0.80}Mg_{0.77}Fe_{0.23}Mn_{0.03})_{\Sigma 1.83}(AsO_4)_2(H_2O_{1.26}OH_{0.74})_2$, are a = 8.925(2) Å, b = 6.143(1) Å, c = 7.352(1) Å, β = 115.25(3)°, ρ_{calc} = 3.73 g/cm^3. The structure of cabalzarite is isomorphic with that of tsumcorite. The site M1 (Ca) is eightfold-coordinated (6 + 2) with average M1-O = 2.549 Å; M2 is octahedral with an average M2-O = 2.010 Å; and the average As-O distance of the arsenate group is 1.689 Å. Charge balance for the simultaneous occupation of M2 by two- and three-valent cations is achieved by H_2O as well as OH contributing to the M2 coordination.

INTRODUCTION

The minerals of the tsumcorite group, of general formula $M1\,M2_2(XO_4)_2(H_2O,OH)_2$, are characterized by a flexible crystal structure, which can accommodate various cations. Natural end-members have been described with Pb, Ca, and Na dominating on the M1 site, Zn, Fe^{3+}, Cu^{2+}, Mn^{3+}, and Co on the M2 site, and As^{5+}, P^{5+}, V^{5+}, and S^{6+} on the X-site. The basic tsumcorite type structure is monoclinic (*C2/m*). Some members display a triclinic cell; the symmetry reduction (Krause et al. 1998) is due to cation ordering on the two M2 positions [e.g., gartrellite, $Pb(Cu,Fe^{3+})_2(AsO_4)_2(H_2O,OH)_2$], or, in the case of species with two H_2O per formula unit (pfu), to the ordering of the hydrogen bonds [e.g., helmutwinklerite, $Pb(Zn,Cu)_2(AsO_4)_2(H_2O)_2$].

This paper reports the occurrence of the first member of the tsumcorite group containing Mg and Al as dominant M2 cations. The mineral occurs in the abandoned Mn-mine of Falotta, Graubünden, Switzerland, and has been named *cabalzarite* as a tribute to Walter Cabalzar, a keen amateur collector who performed an important contribution to the mineralogy of the canton Graubünden (e.g., Bächtiger et al. 1972; Geiger and Cabalzar 1989; Brugger et al. 1994), and who in particular participated in the description of two new minerals from Falotta (grischunite and geigerite). The holotype material is deposited at the "Musée Cantonal de Géologie," Lausanne, Switzerland (sample MGL73785 corresponding to CABA 11 in this paper), and a co-type at the "Naturhistorisches Museum," Basel, Switzerland.

OCCURRENCE

A small Mn-deposit was excavated at the Falotta mine during World War II. Falotta belongs to the numerous Mn-occurrences embedded in the radiolarites, which overlay the MORB-basalts of the Platta Nappe in the Swiss Alps (Geiger 1948). A syn-sedimentary exhalative origin in connection with the Jurassic oceanic ridge volcanism is proposed for these deposits (Suana 1984). The sedimentary ores recrystallized during the regional Alpine metamorphism under lowest greenschist facies conditions (≤325 °C, 3–5 kb; Mählmann 1996; Mählmann, written communication). The ore today consists mainly of braunite, rhodonite, and spessartine. In addition, tinzenite, parsettensite, sursassite, and strontian piemontite are locally abundant.

An As-anomaly is well established in syn-genetic deposits of exhalative hydrothermal origin (Marchig et al. 1982). Many metamorphic equivalents of this type of deposit are famous for

*E–mail: joelb@mail.earth.monash.edu.au.

their As-minerals: examples include Långban, Sweden (Boström et al. 1979), Kombat mine, Namibia (Dunn 1991), Franklin, New Jersey, USA (Dunn 1995), and, in the Alps, the carbonate-hosted deposits of Val Ferrera (Brugger and Berlepsch 1997) and the radiolarite-hosted deposits of Val Graveglia, Italy (Cortesogno et al. 1979). At Falotta, As-bearing minerals occur in several types of veins, which are discordant relative to the main Alpine schistosity. The types are:

(1) Massive brandtite/sarkinite veinlets with minor manganberzeliite and grischunite (type locality; Graeser et al. 1984);

(2) Small open fractures containing free crystals of tilasite, kemmlitzite, bergslagite, and geigerite (type locality; Graeser et al. 1989), together with quartz and albite; and

(3) Thin open fractures and quartz or carbonate veinlets, which occur in a very altered, cohesion-poor ore, and which host cabalzarite.

Cabalzarite results, like the other As-minerals of Falotta, from the hydrothermal remobilization of As during the retrogradation of the Alpine metamorphism.

Appearance and mineral association

Although the occurrence of cabalzarite is restricted to a 1 m^2 outcrop in the Falotta mine, the mineral displays a broad range of morphologies.

(1) Isolated crystals up to 1 mm in size. The largest crystals look like axinite (hatchet-like habitus), and their faces are often curved. In polarized light, most of these crystals show undulatory extinction, and even tiny crystals or fragments of larger crystals usually are unsuitable for single-crystal X-ray investigations. Under the scanning electron microscope (SEM), rare tabular crystals flattened on (001) with a prism and two pinacoids are recognized (Fig. 1).

(2) Complex polycrystalline aggregates, up to 2 mm in length, located in vugs.

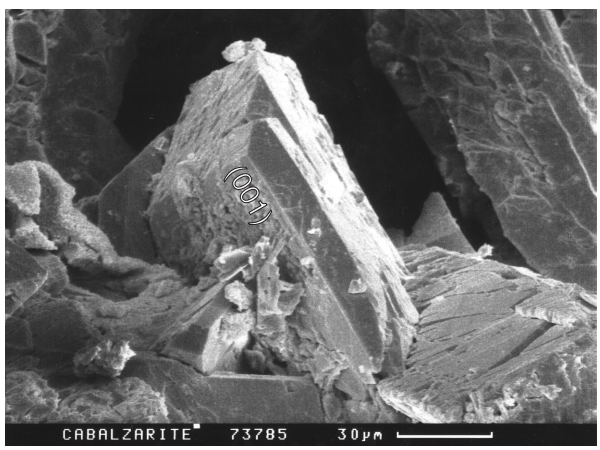

Figure 1. Secondary electron picture of idiomorphic cabalzarite crystals in a vug (holotype sample CABA11)

(3) Fibrous to tabular crystals up to 3 mm in length, forming radiating aggregates up to 5 mm in diameter. These aggregates are developed in two dimensions within thin fractures, and form spheroids where sufficient space was available.

(4) Aggregates of parallel needles filling veinlets up to 2 mm thick, associated with massive quartz, carbonate, and fibrous sursassite. Under this habitus, cabalzarite may be mistaken for the silicate sursassite.

In vugs, cabalzarite is associated with crystals of quartz, adularia, kutnohorite, tilasite $CaMgAsO_4F$, grischunite $NaCa_2Mn_4(Mn^{2+},Fe^{3+})_2(AsO_4)_6 \cdot 2H_2O$, and arseniosiderite $Ca_2Fe_3O_2(AsO_4)_3 \cdot 3H_2O$, with sprays of fine needles of tripuhyite, $FeSbO_4$, and with black crusts of Mn-oxy-hydroxides (rancieite-takanelite). Arsenogoyazite, $(Sr,Ca,Ba)Al_3(AsO_4)(AsO_3OH)(OH)_6$, is apparently a common but easily overlooked mineral associated with cabalzarite: it occurs as xenomorphic grains in cabalzarite, as white veinlets up to several millimeters in width, and as rare pseudo-rhombohedral crystals in vugs.

The sample numbers used in this study refer to small hand specimen (typically $2 \times 3 \times 2$ cm^3). Decimal numbers design different crystals or aggregates picked from the same hand specimen (for example, 11.5 is the crystal from sample 11 for which a crystal structure analysis has been conducted). Most samples contain free crystals and aggregates in vugs. Exceptions are 13 and 14 (radiated aggregates) and 15 (needles filling veinlets).

Physical and optical properties

The physical properties of cabalzarite are summarized in Table 1. The optical properties were difficult to measure, because transparent material was found to be optically very inhomogeneous (oblique or mosaic extinction), which is also related to the strong chemical inhomogeneity of cabalzarite (see below).

Table 1. Physical properties of cabalzarite

$Density_{meas}$*	3.89(3) g/cm^3
$Density_{calc}$†	3.64–3.86 g/cm^3
Color	light-brownish to brownish pink; orange-brown for some isolated crystals
Streak	colorless
Luster	vitreous; transparent, non-fluorescent (UV)
Pleochroism	none observed
$n_{\parallel \text{ fiber elongation}}$‡	1.76 (1)
$n_{\text{perp. fiber elongation}}$‡	1.70 (1)
$n_{mean\ calc}$§	1.77 (6)
Fracture	irregular
Cleavage	none observed
Hardness (Vicker's)	load 50 g, mean VHN 429 kg/mm^2, range 418–447 kg/mm^2, n = 4
Mohs' hardness (after Vicker's)	~5
Twinning	Not observed. Frequent intergrowths around [010].

* Grains from CABA11 immersed in a tube with a density gradient (Clerici solution: Tl formate/Tl malonate/water system). The isodensity solution at the level of the crystal has been sampled using a fine chromatography syringe, and its density deduced from its refractive index.
† From EMP chemical analyses, with a cell volume of 366.3 $Å^3$ (first column in Table 4).
‡ Immersion method.
§ Gladstone-Dale relationship, constants after Mandarino (1976), for the range of compositions obtained by EMP.

CHEMISTRY

The chemical composition of cabalzarite (Table 2) was determined using a JEOL JXA-8600 electron microprobe (EMP) operated at 15 kV, 10 nA, and scanning a surface of 15 μm^2 with a point focused beam. The following standards, X-ray lines and detector crystals were used for calibration: adamite (As*L*α/TAP), graftonite (Fe*K*α/LIF, Mn*K*α/LIF), jadeite (Si*K*α/TAP), olivine (Mg*K*α/TAP), sillimanite (Al*K*α/TAP), strontianite (Sr*K*α/PET), and wollastonite (Ca*K*α/PET). Elements present in minor amounts (0.05 to 0.5 wt% oxide) are V, P, Ba, Na, and Pb. No additional element with atomic number ≥9 was detected; Co, Ni, and Zn in particular are below 0.1 wt% oxide. The presence of H atoms in the mineral is confirmed by an IR spectrum, which shows a broad absorption band between 3690 and 3000 cm^{-1} (O-H stretching mode). An absorption band at 1628 cm^{-1} can be attributed to the bending mode of H_2O, thus indicating that at least part of the hydrogen occurs as H_2O groups. A thermogravimetric analysis (CABA14) has been conducted on a computerized PERKIN ELMER TGS-2 thermobalance with a sensitivity better than 0.1%. The experiments were conducted with 3.30 mg of relatively pure cabalzarite powder (≤1 vol% impurities as determined under the polarization microscope) placed in an open gold sample crucible under dry N_2 atmosphere (to avoid any oxidation), and heated at a 10 °C per minute rate up to 900 °C. The measured weight loss of about 6%, which occurs in one step between 640 and 700 °C, is within the range of the H_2O values calculated from the EMP analyses (5.87–7.30 wt%).

The sums of the EMP analyses are often too low even after the addition of the stoichiometric wt% H_2O, and the M2 site is often underpopulated (Table 2). The low sums and the vacancies on the M2 site are apparently not correlated with other chemical parameters. The M2-vacancies were not confirmed by the crystal structure refinements. These features are probably related to beam-induced damages, which were observed on some samples, to the choice of the EMP standards, and to the poor quality of the sample polish. In spite of these problems, the EMP analyses were normalized on the basis of two (As + Si) pfu. From similarity with the other members of the tsumcorite group containing either Fe^{3+} (e.g., ferrilotharmeyerite) or Mn^{3+} (e.g., lotharmeyerite), and in accord with the association with Fe^{3+} minerals (tripuhyite, arseniosiderite), all Fe and Mn were considered to be trivalent. The OH/H_2O ratio was then calculated to obtain a total of ten O atoms pfu.

Backscattered electron (BSE) images reveal chemical zoning in most grains. Idiomorphic crystals (Fig. 2) display complex growth zonations, sometimes with changing of morphology in the course of the crystallization (arrow 1 in Fig. 2). Furthermore, the crystals appear to have been broken at some stage of their geological history (arrows 2 and 3 in Fig. 2). Both features together explain the poor optical quality of the crystals. BSE images of fibrous cabalzarite often reveal a fine patchy zoning.

The EMP analyses show that the chemical variability of cabalzarite occurs mainly on the M2 site, and involves Mg, Al, Fe, and to a lesser extend Mn. In a Mg-Fe-Al triangular projection (Fig. 3), the analyses are distributed almost equally between the Mg and Al fields, and some approach the triple point. No analysis, however, plots in the Fe^{3+} field corresponding to ferrilotharmeyerite.

TABLE 2. Chemical analyses of cabalzarite

Sample number	11.5*	11.3	13.2	15.1	10	20*	MIN	MAX
No. of analyses	4	3	5	6	4	15	92	
As_2O_5	55.57	52.25	52.92	52.83	53.48	53.31	50.96	56.14
SiO_2	0.05	0.14	0.77	1.32	0.87	0.75	<0.05	1.87
Al_2O_3	9.84	5.13	10.46	10.50	8.96	9.85	4.52	11.51
MgO	7.54	7.58	7.22	6.65	6.99	7.61	5.71	8.88
Fe_2O_3	4.38	11.23	<0.04	1.61	3.75	1.54	<0.04	11.40
Mn_2O_3	0.55	0.73	3.88	4.29	3.74	4.90	0.32	5.21
SrO	0.49	0.32	0.51	0.61	0.46	0.33	0.03	0.94
CaO	13.64	13.67	13.65	13.88	13.88	12.63	12.02	15.53
BaO	n.d.	0.13	0.17	0.04	0.18	n.d.	<0.04	0.49†
H_2O_{calc}	7.11	5.99	6.86	6.76	6.77	6.63	5.87	7.30
Sum	99.17	97.17	96.44	98.49	99.08	97.55	96.03	100.51
As	2.00	1.99	1.95	1.91	1.94	1.95	1.87	2.00
Si	0.004	0.01	0.05	0.09	0.06	0.05		0.13
Sum	2.00	2.00	2.00	2.00	2.00	2.00	2.00	2.00
Sr	0.02	0.01	0.02	0.03	0.02	0.01	0.001	0.04
Ba		0.00	0.005	0.001	0.005			0.04
Ca	1.00	1.07	1.03	1.03	1.03	0.95	0.90	1.16
∑M1	1.02	1.08	1.05	1.06	1.05	0.96	1.00	1.21
Al	0.80	0.44	0.87	0.86	0.73	0.81	0.39	0.94
Fe^{3+}	0.23	0.62		0.08	0.20	0.08		0.62
Mg	0.77	0.82	0.76	0.69	0.72	0.79	0.62	0.93
Mn^{3+}	0.03	0.04	0.21	0.23	0.20	0.26	0.02	0.28
∑M2	1.83	1.92	1.84	1.86	1.85	1.94	1.75	1.97
OH‡	0.74	1.09	0.79	0.88	0.87	0.91	0.60	1.18
H_2O‡	1.26	0.91	1.21	1.12	1.13	1.09	0.82	1.40
O_{tot}‡	10.00	10.00	10.00	10.00	10.00	10.00	10.00	10.00

* CABA11.5 is the crystal used for crystal structure analysis at Lausanne. CABA20 are grains collected close to the crystal used for crystal structure analysis at Bern, which itself could not be successfully prepared for EMP analysis. The analyses are normalized on the basis of As + Si = 2.00. The following elements were detected only in minor amounts: V_2O_5 (≤0.15 wt%), P_2O_5 (≤0.11 wt%), Na_2O (≤0.08 wt%), PbO ≤0.12 wt%.

† One analysis with 1.50 wt% BaO has been omitted.

‡ The H_2O and OH contents are calculated to obtain a total of 10 O pfu, assuming that all Fe and Mn is trivalent, and $(OH + H_2O) = 2$.

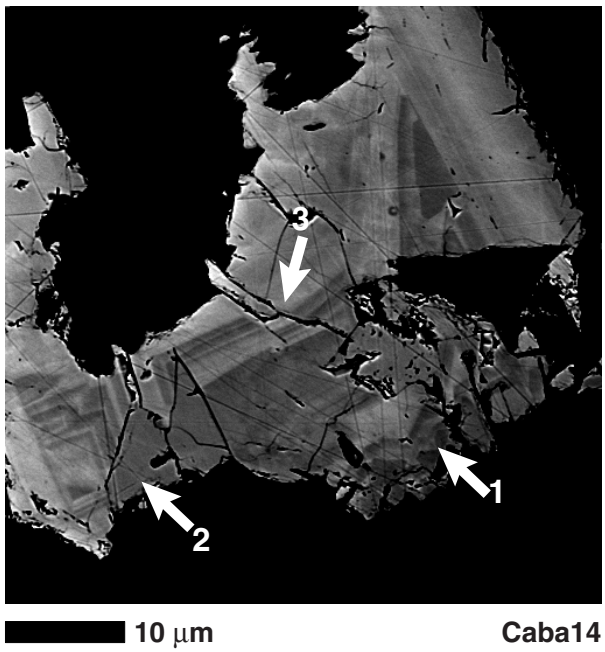

FIGURE 2. Backscattered electron image of a cabalzarite crystal showing a complex growth zoning, apparently accompanied by changing of crystal morphology during growth (arrow 1) and post-crystallization stresses (arrows 2 and 3).

The excellent negative correlation between Al and Mg + Fe + Mn (Fig. 4a) is consistent with the occurrence of these elements on a single crystallographic site. Figure 4b shows that the major chemical variability in cabalzarite is related to the $Al^{3+}Fe^{3+}_{-1}$ exchange vector (see also Fig. 3). The Mn^{3+} content of cabalzarite does not exceed 0.28 pfu, although cabalzarite occurs in Mn-rich ores; Al- and Mn-rich cabalzarite may be distinguished from an Al- and Mn-poor population (Fig. 4c).

X-RAY POWDER DIAGRAM

The X-ray powder pattern of sample CABA11 was determined with a 500 mm diameter diffractometer with Debye-Scherrer geometry at the European Synchrotron Research Facility in Grenoble, using a 0.3 mm diameter capillary tube containing about 0.14 mm^3 of cabalzarite powder (Tables 3 and 4). The differences in the volumes of the cells refined from the powder data and from single crystal measurements can be explained by the chemistry of the M2 site, and in particular by the different $(Fe^{3+} + Mn^{3+})/Al^{3+}$ proportions on this site (ionic radius of octahedral Fe^{3+} (High Spin) = 0.645 Å, Mn^{3+} = 0.645 Å, Al^{3+} = 0.535 Å; Shannon 1976). For example, the composition of the single crystal CABA11.5 is Fe-poor and Al-rich in comparison to that of the other analyzed crystals from CABA11 (Figs. 3, 4b, and 4c; Table 2). The cell volume of the single crystal CABA11.5 is 0.5% smaller than that retrieved from bulk cabalzarite in CABA11 (Table 4), as expected from simple ionic radius considerations. The cell volume of ferrilotharmeyerite, with Fe^{3+} and Zn on the M2 site ($^{[VI]}Zn$ = 0.74 Å, compared to $^{[VI]}Mg$ = 0.72 Å) is about 3% larger than that of cabalzarite.

CRYSTAL STRUCTURE

Preliminary studies using a Weissenberg camera revealed the difficulty to select a crystal of suitable quality for crystal structure analysis because most crystals displayed very diffuse or multiple reflections. Two small cabalzarite crystals could, however, be successfully measured on image plate and CCD detectors at Lausanne (CABA11.5) and Bern (CABA20), respectively. Details of data collection and structure refinement are listed in Table 5, the structural parameters in Table 6, and inter-atomic bond distances and bond-valence calculations for cabalzarite and ferrilotharmeyerite in Table 7. The two structures were refined independently, but the final results are in excellent agreement.

Structure solution and refinement of the CABA20 crystal was carried out with the SHELX-97 program package (Sheldrick 1997) applying neutral atom scattering factors. An

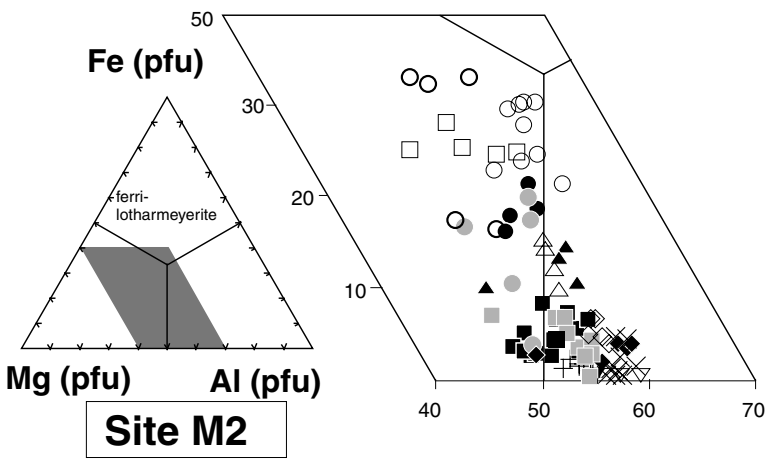

FIGURE 3. Triangular projection of the main M2-cations in cabalzarite. Both Al- and Mg-rich compositions are found, and some analyses approach the Fe-field. See Figure 4 for the symbols.

TABLE 3. X-ray data on cabalzarite (CABA11)

h	*k*	*l*	I_{calc}*	d_{calc}	d_{meas}	I_{meas}
0	0	1	0.2	6.653	6.652	1
1	1	0	46	4.898	4.895	59
$\bar{1}$	1	1	32	4.546	4.544	35
2	0	0	5	4.043	4.041	3
1	1	1	14	3.532	3.533	16
$\bar{2}$	0	2	47	3.371	3.373	54
0	0	2	3	3.327	3.327	2
$\bar{1}$	1	2	100	3.158	3.159	100
0	2	0	37	3.078	3.078	32
2	0	1	60	2.942	2.942	67
0	2	1	27	2.793	2.794	31
3	1	$\bar{1}$	55	2.682	2.684	55
2	2	$\bar{1}$	52	2.519	2.519	81
3	1	$\bar{2}$	27	2.507	2.510	33
1	1	2	31	2.471	2.471	32
3	1	0	3	2.469		
$\bar{2}$	2	2	6	2.273	2.273	6
1	1	$\bar{3}$	2	2.251	2.252	5
0	0	3	1	2.217	2.217	2
2	0	2	13	2.156	2.156	13
2	2	1	29	2.127	2.126	26
3	1	1	3	2.066	2.066	3
4	0	0	3	2.021	2.022	2
$\bar{4}$	0	3	6	1.971	1.971	5
$\bar{1}$	3	1	5	1.963	1.963	4
$\bar{2}$	2	3	1	1.908	1.909	1
1	3	1	3	1.853	1.847	22
1	$\bar{1}$	3	20	1.849		
$\bar{2}$	0	4	12	1.839	1.839	14
0	2	3	2	1.799	1.796	3
$\bar{1}$	3	2	12	1.792	1.790	11
2	2	2	3	1.766	1.766	3
3	1	4	2	1.728	1.728	2
1	1	$\bar{4}$	2	1.716	1.715	3
$\bar{5}$	1	2	1	1.715		
3	$\bar{1}$	2	1	1.691	1.691	17
$\bar{3}$	3	1	19	1.690		
4	2	0	5	1.690		
$\bar{5}$	1	1	7	1.686	1.686	22
$\bar{4}$	0	4	13	1.685		

Notes: Diffractometer, synchrotron X-radiation, λ = 1.09816 Å (ESRF Grenoble). Lines/intensity at 4.260/1, 3.256/2, 3.014/1, 2.869/1, 2.739/2, 2.629/1, 2.346/<1, 1.819/1 could not be indexed and are attributed to unknown impurities.

* Intensities calculated for the formula $Ca(MgAl)(AsO_4)_2(OH)(H_2O)$ with the program CrystalDiffract (http//:www.crystalmaker.co.uk).

TABLE 4. Comparison of the unit-cell parameters for cabalzarite and ferrilotharmeyerite

Sample	CABA11*	CABA11.5†	CABA20‡	Ferrilotharmeyrite§
a (Å)	8.945(1)	8.925(2)	8.9284(5)	9.010(3)
b (Å)	6.156(1)	6.143(1)	6.1314(5)	6.246(2)
c (Å)	7.358(1)	7.352(1)	7.3439(6)	7.391(2)
β (°)	115.30(2)°	115.25(3)°	115.494(7)	115.32
V (Å^3)	366.3(1)	364.6(1)	362.9(1)	375.4

* Refined from the Synchrotron powder data (Table 3) using the program UnitCell (Holland and Redfern 1997).
† Single crystal, Image plate detector, Lausanne.
‡ Single crystal, CCD detector, Bern.
§ Ferrilotharmeyrite no. 241 (Krause et al. 1998).

empirical absorption correction was carried out with a psi-scan related method where redundant and symmetry equivalent reflections in the various frames were applied to calculate transmission factors. Test refinements were performed in space groups *C*2, *Cm*, and *C*2/*m*. Subsequent screening of the results indicated that *C*2/*m* symmetry was correct. Prior to this stage the isomorphic relationship with tsumcorite was not recognized. The scattering power on the octahedral M2 site indicated a mixed occupation of transition metals (Fe and Mn) and light elements (Mg and Al). Due to the similarity of Mn and Fe as well as Mg and Al scattering factors the distribution of these elements could not be resolved. As a compromise, the concentration of Mn (simulating Mn and Fe) and Mg (simulating Mg and Al) were allowed to vary. The refined transition metal concentration of 17% is in good agreement with average analyses (CABA20, Table 2) collected on crystals from the same hand specimen. At the final stage of refinement H positions were extracted from difference Fourier maps and restrained to be bonded within 0.95(3) Å to the adjacent oxygen site. Final difference Fourier maps revealed maximum peaks of ±0.5 e/Å^3.

The diffraction pattern of CABA11.5 did not reveal any kind of twinning. Most (85%) of the spots could be explained in the cell given in Table 4, but some of them were somewhat smeared out, mainly in the (**a*,c***) plane, indicating the presence of (010) intergrowths. Regarding the habitus, two pinacoids and one pedion could be identified with confidence: the platelet face {001}, {$2\bar{2}\bar{1}$}, and the {$31\bar{1}$} pedion, but a curved fracture plane was approximated with the help of the {$\bar{2}\bar{2}1$} pedion. These forms were then used to integrate transmission factors using FACEIT (part of STOE IPDS). The structure was easily determined with the help of DirDif (Beurskens et al. 1998) and refined by means of SHELXTL 5.05 (Siemens Analytical Instruments). Mg was chosen to represent Al/Mg and Fe to stand in for Fe/Mn. The refined transition metal percentage is in excellent agreement with the concentration found by the EMP (Table 2). After anisotropic refinement of all non-hydrogen atoms, a difference map was computed ($R_1 \approx 0.019$). Quite a few of the ten highest residua lay near O atoms, so the three strongest ones were tentatively included in the refinement as isotropic H atoms ($R_1 \approx 0.018$). The IDPs of the first and the third residua were reasonable, but the one of the second indicated that this peak had to be considered a ghost or noise. Of the other two, one named H14, lay between O1 and O4 (O1$^{0.73\ Å}$ H14$^{1.90\ Å}$ O4, angle around H14 162°), and the other one, named H11, between O1 and O11$^{\$}$ (O1$^{0.73\ Å}$ H11$^{1.86\ Å}$ O1$^{\$}$), where $ stands for {Ci | 111}. Both these geometries are classical for hydrogen bonds, but because H11 lies too close to H11$^{\$}$, H11 must occupy either the position H11 or H11$^{\$}$, and for this reason it was assigned a population parameter of 0.5. For the refinement, the O-H distances found in the Fourier map and an ideal angle H-O-H were imposed; the IDP of H11 had to be tied to the one of O11. Final difference Fourier maps show maximum peaks of ±0.5 eÅ^{-3}.

Cabalzarite is isostructural with tsumcorite. A detailed description of the topology of this structural type can be found in Tillmanns and Gebert (1973) and Krause et al. (1998). Chains of edge-sharing $M2O_6$ octahedrons, extending along [010], are linked together by AsO_4 tetrahedrons and form layers parallel to (001). The O atoms represent two layers out of a distorted close-packed arrangement. M1$^{[6+2]}$ atoms link these layers. Hydrogen bonds develop within the layers (between two O1 belonging to two octahedral chains), as well as across the layers (between O1 and O4 at the apex of an AsO_4 tetrahedron). The structures of cabalzarite and ferrilotharmeyerite are very similar; the main difference is the size of the M2 octahedron (Table 7).

Bond-valence calculations (Table 7) confirm the attribution of H atoms to O1 and O4, the pentavalent state of As, and the

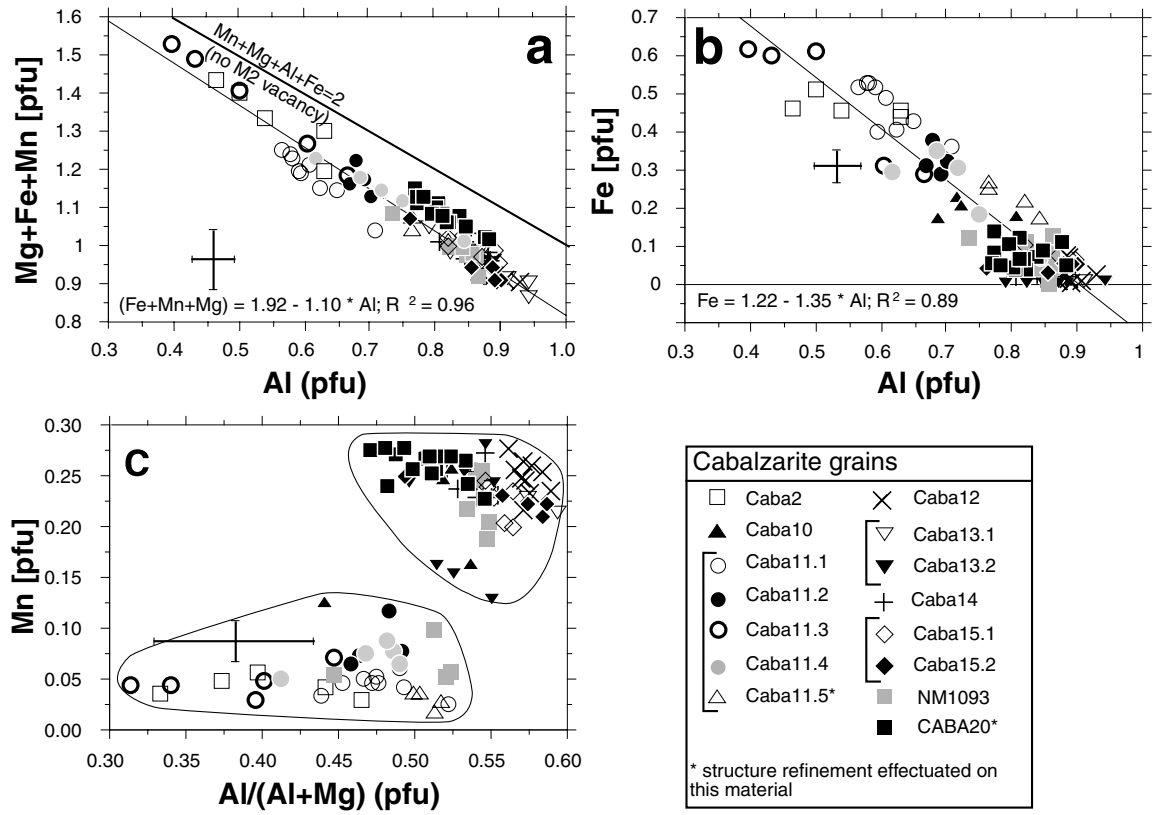

FIGURE 4. Bivariate plots illustrating the chemical composition of cabalzarite. (**a**) Good correlation with a slope near –1 between the M2-cations; (**b**) The largest part of the chemical variability of cabalzarite is related to the $AlFe_{-1}$ exchange vector; (**c**) Mn vs. Al/(Al + Mg) diagram illustrating the two main cabalzarite populations.

TABLE 5. Parameters for crystal structure refinement

	CABA11.5 (Lausanne)	CABA20 (Bern)
Diffractometer	Stoe IPDS	Siemens Smart CCD
X-ray radiation	Mo$K\alpha$ (0.71073 Å)	Mo$K\alpha$ (0.71073 Å)
X-ray power	55 kV, 50 mA	50 kV, 40 mA
Temperature	293 K	293 K
Crystal size	180 × 160 × 60 µm	25 × 25 × 50 µm
Detector to sample distance	6.00 cm	5.18 cm
Detector 2Θ angle	0°	27°
Resolution	0.76 Å	0.77 Å
Rotation axis	ϕ	ω
Rotation width	1.0°	0.3°
Total number of frames	200	1271
Frame size	1200 * 1200 pixels	512 * 512 pixels
Data collection time per frame	6 min.	10 sec.
Collection mode	> hemisphere	automated hemisphere
Reflection collected	1640	1948
Max. 2Θ	56.30	54.89
Index range	$-11 \le h \le 11$, $-7 \le k \le 8$, $-9 \le l \le 9$	$-9 \le h \le 11$, $-4 \le k \le 7$, $-9 \le l \le 9$
Unique reflections	448	415
Reflections > 2σ(*I*)	436	367
R_{int}, after empirical absorp. correct.	–	2.71%
R_{int}, numerical based on habitus	3.43%	–
R_{σ}	1.97%	3.30%
Number of least squares parameters	51	52
GooF	1.241	1.206
R_1, I>2σ(I)	1.80%	1.86%
R_1, all data	2.10%	2.72%
wR_2 (on F^2)	6.65%	4.1

TABLE 6. Final atomic positional parameters, U_{eq} ($\times 10^2$), and anisotropic displacement ($\times 10^2$) parameters for the two cabalzarite crystals investigated. Standard deviations in parentheses

At.	Occ.	*x*	*y*	*z*	U_{eq}	U_{11}	U_{22}	U_{33}	U_{23}	U_{13}	U_{12}
CABA11.5, Lausanne											
[X]As	1	0.91597(3)	1/2	0.20844(3)	0.491(6)	0.36(1)	0.67(1)	0.49(1)	0	0.225(7)	0
[M1]Ca	1	0	0	0	0.90(1)	1.06(2)	0.88(3)	1.00(2)	0	0.67(2)	0
[M2]Al+Mg	0.80(1)	1/4	1/4	1/2	0.40(2)	0.33(2)	0.41(3)	0.38(2)	–0.05(2)	0.07(2)	0.06(2)
[M2]Mn+Fe	0.20(1)	1/4	1/4	1/2							
O1	1	0.3401(1)	1/2	0.4089(1)	1.02(4)	0.67(6)	1.82(8)	0.60(6)	0	0.31(5)	0
O2	1	0.3168(2)	0	0.3648(2)	0.98(3)	0.78(5)	1.33(8)	1.13(6)	0	0.71(5)	0
O3	1	0.0371(1)	0.2771(2)	0.2519(2)	0.84(3)	0.78(4)	0.75(5)	1.03(4)	0.04(4)	0.39(3)	0.11(1)
O4	1	0.2402(2)	1/2	0.0187(2)	1.40(4)	0.86(6)	2.4(1)	0.65(6)	0	0.01(5)	0
H11*	0.5	0.4278(1)	1/2	0.4785(2)	1.5(1)						
H14*	1	0.3321(3)	1/2	0.3058(1)	5.2(1)						
CABA20, Bern											
[X]As	1	0.91648(6)	1/2	0.20931(7)	0.92(2)	0.81(3)	1.09(3)	0.86(3)	0	0.38(2)	0
[M1]Ca	1	0	0	0	1.54(4)	1.83(7)	1.43(7)	1.60(7)	0	0.96(6)	0
[M2]Al+Mg	0.83(1)	1/4	1/4	1/2	1.00(4)	1.00(6)	1.06(7)	1.16(6)	0.00(4)	0.39(5)	0.04(4)
[M2]Mn+Fe	0.17(1)	1/4	1/4	1/2							
O1	1	0.3396(4)	1/2	0.4103(4)	1.66(8)	1.1(2)	2.5(2)	1.3(2)	0	0.51(1)	0
O2	1	0.3169(4)	0	0.3636(4)	1.74(8)	1.7(2)	2.2(2)	1.7(2)	0	1.1(1)	0
O3	1	0.0376(2)	0.2764(4)	0.2528(3)	0.15(6)	1.5(1)	1.3(1)	1.7(1)	–0.04(9)	0.68(9)	0.1(1)
O4	1	0.2385(4)	1/2	0.0186(4)	2.13(8)	1.8(2)	2.9(2)	1.3(2)	0	0.2(1)	0
H11*	0.5	0.450(6)	1/2	0.43(2)	7(5)						
H14*	1	0.294(6)	1/2	0.270(4)	3(1)						

* Starred atoms were refined isotropically.

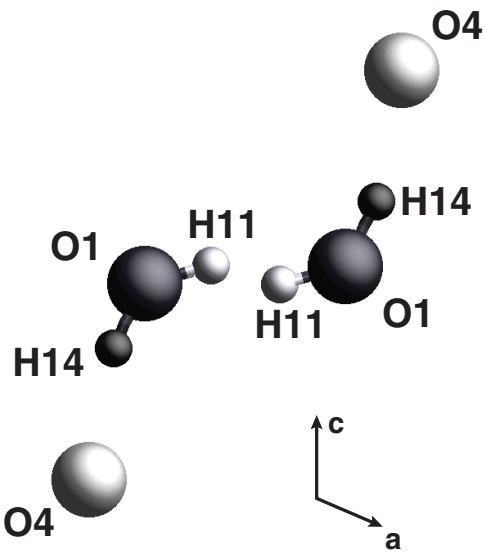

FIGURE 5. Detail of the hydrogen bonding scheme [projection on (010)] as refined from the structure refinements of CABA11.5 and CABA20. Notice that H11 is only 50% occupied. See text for discussion.

TABLE 7. Interatomic distances (Å) and bond-valence sums (v) for cabalzarite and ferriltharmeyerite

	Ferriltharmeyerite*		CABA11.5	
	d	v	d	v
M1-O2 2×	2.962(2)	0.07	2.952(2)	0.07
M1-O3 4×	2.441(2)	0.28	2.432(2)	0.29
M1-O4 2×	2.386(2)	0.32	2.381(2)	0.33
Mean	2.558	1.90	2.549	1.96
M2-O1 2×	2.027(1)	0.45	1.9783(7)	0.46
M2-O3 2×	2.052(1)	0.42	2.002(2)	0.44
M2-O2 2×	2.097(1)	0.37	2.051(2)	0.38
Mean	2.059	2.48	2.010	2.56
X-O2	1.726(2)	1.12	1.724(2)	1.13
X-O3 2×	1.692(1)	1.23	1.688(2)	1.24
X-O4	1.658(2)	1.34	1.657(2)	1.34
Mean	1.692	4.92	1.689	4.95
O1...O1	2.543(2)		2.584(3)	
O1...O4	2.607(3)		2.616(5)	
O1-H11			0.73(3)	
O1-H14			0.73(3)	
H11-O1-H14			109.2(2)	
O1...O1...O4	111.58(8)°		110.83(7)°	

Notes: Σv for the O atoms, without consideration of the H atoms, for cabalzarite (CABA11.5/CABA20): O1-0.93/0.98, O2-1.96/2.00, O3-1.96/1.98, O4-1.67/1.68. Bond valence parameters from Altermatt and Brown (1985).

* From Krause et al. (1998).

mixed valence on the site M2. The M^{2+} / M^{3+} ratio (M^{2+} = Mg, M^{3+} = Al + Fe + Mn) in cabalzarite lies between 0.52 and 0.99. The $M^{2+}M^{3+}_{-1}$ substitution in M2 is balanced according to the coupled substitution:

$$M^{2+} + H_2O = M^{3+} + OH^-$$

This substitution has been first recognized in tsumcorite by Tillmanns and Gebert (1973) and later confirmed by Krause et al. (1998). For species with $M^{2+}/M^{3+} = 1$, the following bonding scheme may form:

$$\begin{array}{c} O4 \ldots H14 - O1 - H11 \ldots O1 - H14 \ldots O4 \\ \mathbf{c} \\ O4 \ldots H14 - O1 \ldots H11 - O1 - H14 \ldots O4 \end{array}$$

This corresponds to the $H_3O_2^-$ unit (Chevrier et al. 1990; Chevrier et al. 1993; Beran et al. 1997). The positions of hy-

drogen atoms refined from the crystals CABA11.5 and CABA20 confirm the bonding scheme described above (Fig. 5). H14 is located near O1 and points toward O4. The H11 positions are located between two neighboring O1 atoms (O1-O1 distance of 2.584 Å), and only one of the two H11 sites between each O1-O1 pair can be occupied simultaneously. A better understanding of the hydrogen bonding in cabalzarite must await the acquisition of high resolution IR-spectra on this mineral.

NOMENCLATURE

Cabalzarite is a typical example of a mineral causing a classification problem because it lies in the middle of a solid solution series: strictly speaking, both Mg^{2+} and Al^{3+} were found to dominate the M2-site (Al/Mg = 0.69–2.21; Fig. 3). Most analyses, however, scatter along the Al:Mg = 1:1 line, and no crystal approaching Al- or Mg-endmember composition could be isolated. Thus, according to the IMA guidelines, the use of two different names is not justified (Nickel 1992). We have chosen to define cabalzarite as $Ca(Mg,Al,Fe,Mn)_2(AsO_4)_2(H_2O,OH)_2$ because cabalzarite sample CABA11, on which most work has been conducted, plots in the Mg-field. The crystal CABA11.5 submitted to crystal-structure analysis furnished the only analyses for this sample that plot in the Al field, but the Mg/Al ratio of this crystal is very close to 1.00 (0.94–1.00, mean = 0.97). The crystal from CABA20 analyzed in Bern most likely also has a Mg/Al ratio close to one (Fig. 3; Table 2).

ACKNOWLEDGMENTS

Thanks to Uwe Kolitsch (Museum of Natural History, Adelaide) for interesting discussions, and to Werner Krause (Hürth, Germany) for providing us a pre-print of his paper about the tsumcorite group. Thomas Mummentaler (Zürich), Hans-Peter Klinger (Jona) and Walter Cabalzar (Chur) kindly provided cabalzarite samples. Stefan Graeser (Institute for Mineralogy, University of Basel) measured the micro-hardness of cabalzarite. Our thanks are also due to A. Geoffroy and A. Burkhard (both Novartis Services AG, Basel) for performing the thermogravimetric measurements. We take great pleasure in acknowledging the staff of the Swiss-Norwegian Beam Lines at ESRF for help during data collection, and Philippe Thélin (Institute of mineralogy and geochemistry, University of Lausanne) and Peter O. Baumgartner (Institute of geology and paleontology, University of Lausanne) for facilitating access to their laboratories. The manuscript benefited from the insightful comments of Jefferey E. Post and an anonymous reviewer.

REFERENCES CITED

Altermatt, D. and Brown, I.D. (1985) Bond-valence parameters obtained from a systematic analysis of the inorganic crystal structure database. Acta Crystallographica, B41, 244–248.

Bächtiger, K., Rüdlinger, G., and Cabalzar, W. (1972) Scheelit in Quarz- und Fluorit-Gängen am Calanda (Kt. Graubünden). Schweizerische Mineralogische und Petrographische Mitteilungen, 52, 561–563.

Beran, A., Giester, G., and Libowitzky, E. (1997) The hydrogen bond system in natrochalcite-type compounds—an FTIR spectroscopic study of the $H_3O_2^-$ unit. Mineralogy and Petrology, 61, 223–235.

Beurskens, P.T., Beurskens, G., de Gelder, R., Garcia-Granda, S., Gould, R.O., Israel, R., and Smits, J.M.M. (1998) The DIRDIF-99 program system. Crystallography Laboratory, University of Nijmegen, The Netherlands.

Boström, K., Rydell, H., and Joensuu, O. (1979) Långban—an exhalative sedimentary deposit? Economic Geology, 74, 1002–1011.

Brugger, J. and Berlepsch, P. (1997) Johninnesite $Na_2(Mn^{2+})_9(Mg,Mn)_7(AsO_4)_2(Si_6O_{17})_2(OH)_8$: a new occurrence in the Val Ferrera (Graubünden, Switzerland). Schweizerische Mineralogische und Petrographische Mitteilungen, 77, 449–455.

Brugger, J., Cabalzar, W., and Weibel, M. (1994) Neufund: Romeit in den Schweizer Alpen. Mineralienfreund, 4, 1–7.

Chevrier, G., Giester, G., Jarosch, D., and Zemann, J. (1990) Neutron diffraction study of the hydrogen-bond system in $Cu_2K(H_3O_2)(SO_4)_2$. Acta Crystallographica, C46, 175–177.

Chevrier, G., Giester, G., and Zemann, J. (1993) Neutron refinements of $RbCu_2(H_3O_2)(SO_4)_2$ and $RbCu_2(H_3O_2)(SeO_4)_2$: variation of the hydrogen bond system in the natrochalcite type series. Zeitschrift für Kristallographie, 206, 7–14.

Cortesogno, L., Lucchetti, G., and Penco, A.M. (1979) Le mineralizzazioni a manganese nei diaspri delle ofioliti liguri: mineralogia e genesi. Rendiconti della Societa Italiana di Mineralogia e Petrologia, 35, 151–197.

Dunn, P. (1995) Franklin and Sterling Hill, New Jersey: the World's Most Magnificent Mineral Deposit.

Dunn, P.J. (1991) Rare minerals of the Kombat mine, Namibia. Mineralogical Record, 22(6), 421–424.

Geiger, T. (1948) Manganerz in den Radiolariten Graubündens. Beiträge zur Geologie der Schweiz, Geotechnische Serie, 27, 89 p.

Geiger, T. and Cabalzar, W. (1989) Ardennit—ein Neufund von der Alp Parsettens, Val d'Err, GR. Schweizer Strahler, 8, 201–211.

Graeser, S., Schwander, H., and Suhner, B. (1984) Grischunit ($CaMn_2[AsO_4]_2$), eine neue Mineralart aus den Schweizer Alpen. Schweizerische Mineralogische und Petrographische Mitteilungen, 64, 1–10.

Graeser, S., Schwander, H., Bianchi, R., Pilati, T., and Gramaccioli, C.M. (1989) Geigerite, the Mn analogue of chudobaite: Its description and crystal structure. American Mineralogist, 74, 676–684.

Holland, T.J.B. and Redfern, S.A.T. (1997) Unit cell refinement from powder diffraction data: the use of regression diagnostics. Mineralogical Magazine, 61, 65–77.

Krause, W., Belendorff, K., Bernhardt, H.-J., McCammon, C., Effenberger, H., and Mikenda, W. (1998) Crystal Chemistry of the tsumcorite-group minerals. New data on ferrilotharmeyerite, tsumcorite, thometzekite, mounanaite, helmutwinklerite, and a redefinition of gartrellite. European Journal of Mineralogy, 10, 179–206.

Mählmann, R.F. (1996) Das Diagenese-Metamorphose-Muster von Vitrinitreflexion und Illit-"Kristallinität" in Mittelbünden und im Oberhalbstein. Teil 2: Korrelation kohlenpetrographischer und mineralogischer Parameter. Schweizerische Mineralogische und Petrographische Mitteilungen, 76, 23–45.

Mandarino, J.A. (1976) The Gladstone-Dale relationship. Part I: derivation of new constants. Canadian Mineralogist, 14, 498–502.

Marchig, V., Gundlach, H., Moller, P., and Schley, F. (1982) Some geochemical indicators for discrimination between diagenetic and hydrothermal metalliferous sediments. Marine Geology, 50, 241–256.

Nickel, E.H. (1992) Solid solutions in mineral nomenclature. Mineralogical Magazine, 56, 127–130.

Shannon, R.D. (1976) Revised effective ionic radii and systematic studies of interatomic distances in halides and chalcogenides. Acta Crystallographica, A32, 751–767.

Sheldrick, G.M. (1997) SHELX-97, program for crystal structure determination. University of Göttingen, Germany.

Suana, M. (1984) Die Manganerzlagerstätten von Tinizong (Oberhalbstein, Graubünden). Beiträge zur Geologie der Schweiz, Geotechnische Serie, 64, 94 p.

Tillmanns, E. and Gebert, W. (1973) The crystal structure of tsumcorite, a new mineral from the Tsumeb Mine, S.W. Africa. Acta Crystallographica, B29, 2789–2794.

MANUSCRIPT RECEIVED OCTOBER 21, 1998
MANUSCRIPT ACCEPTED MARCH 16, 2000
PAPER HANDLED BY JAMES W. DOWNS